



HAL
open science

On isotropic circular arrays of anisotropic sensors

Houcem Gazzah, Jean-Pierre Delmas

► **To cite this version:**

Houcem Gazzah, Jean-Pierre Delmas. On isotropic circular arrays of anisotropic sensors. ISSPIT 2015: International Symposium on Signal Processing and Information, Dec 2015, Abu Dhabi, United Arab Emirates. pp.95-99, 10.1109/ISSPIT.2015.7394427. hal-01256700v1

HAL Id: hal-01256700

<https://hal.science/hal-01256700v1>

Submitted on 15 Jan 2016 (v1), last revised 5 Apr 2016 (v2)

HAL is a multi-disciplinary open access archive for the deposit and dissemination of scientific research documents, whether they are published or not. The documents may come from teaching and research institutions in France or abroad, or from public or private research centers.

L'archive ouverte pluridisciplinaire **HAL**, est destinée au dépôt et à la diffusion de documents scientifiques de niveau recherche, publiés ou non, émanant des établissements d'enseignement et de recherche français ou étrangers, des laboratoires publics ou privés.

ON ISOTROPIC CIRCULAR ARRAYS OF ANISOTROPIC SENSORS

Houcem Gazzah

Dept. of Elec. and Computer Engineering
University of Sharjah, 27272, UAE
hgazzah@sharjah.ac.ae

Jean Pierre Delmas

Samovar lab, Telecom SudParis, CNRS
Université de Paris Saclay, 91011 Evry, France
jean-pierre.delmas@it-sudparis.eu

ABSTRACT

Uniform circular arrays are popular in direction finding applications because they show to be isotropic, i.e. they exhibit the same accuracy (in terms of the Cramer-Rao bound) at all possible planar look directions. We prove that this is not absolutely true if the constituent sensors are not isotropic. For instance, we specify how the anisotropic sensors should be directed and how many are needed in order to ensure an isotropic behavior of the array. We study, in more details, the performance of arrays of cardioid sensors, including anisotropic arrays of cardioid sensors.

Index Terms— Cramer Rao bounds, direction-of-arrival estimation, Cardioid sensors

1. INTRODUCTION

Estimating the direction-of-arrival (DOA) of a remote source is best achieved by means of arrays of sensors. Snapshots delivered by the sensors differ in phase, in a way that depends on the source DOA. In the single source case, most estimation algorithms achieve (near) optimality, i.e., achieve a Mean Square Error (MSE) close to the so-called Cramer-Rao Bound (CRB). These include the *high-resolution* MUSIC algorithm [1] and the *low-resolution* beam-forming algorithm [2].

In general, estimation accuracy is different from a look direction to another, and this depends on the way sensors are placed. Only some array geometries will lead to the same accuracy at all possible planar look azimuth directions, forming the so-called isotropic arrays. This is a very desired property of antenna arrays, especially for surveillance applications [3]. Such arrays include the (trivial and very popular) Uniform Circular Array (UCA) [4] and the (less trivial and more recent) V array [5]. However, it should be mentioned that the CRB has been proved to be azimuth-independent only in the case of arrays of omni-directional sensors [5].

Following a plausible intuition, a UCA of anisotropic (directional) sensors is still isotropic if the constituent sensors are pointed in the direction center-to-sensor [4, 6, 7]. This is suggested by the apparent circular symmetry of so-disposed array. However, because of the finite number of sensors, the UCA is not rotationally-invariant, as will be clarified in this

paper. Formally, we prove that the UCA is not isotropic until a sufficient number of sensors is deployed. We give the exact minimum required number of sensors and the exact expression of the so-achieved DOA-independent CRB.

The paper is organized as follows. In Sec. 2, we introduce the observation model and develop expressions of the CRB. In Sec. 3, we address UCAs of directive sensors of a particular geometry that is often reported in the literature as being isotropic. We attenuate these claims and show additional requirements for this to be true. For illustration purposes, we study in details the case of arrays of cardioid sensors. Finally, a conclusion is given in Sec. 4.

2. SIGNAL MODEL

A number of M sensors is deployed in the $[O, x, y]$ plane to form an antenna array. Sensor m is located at point P_m , at a distance $OP_m = \rho_m \lambda$ from the origin O and such that $[O, P_m)$ forms an angle ϕ_m with the $[O, x)$ axis. A far-field coplanar source is pointing at the array from the angle θ , measured counter-clockwise from $[O, x)$. It is emitting a narrow-band signal $s(t)$ of wavelength λ in the direction of the array, so that the array delivers, at time index t , a vector-valued output

$$\mathbf{x}(t) = \mathbf{a}(\theta)s(t) + \mathbf{n}(t)$$

proportional (but noise-corrupted) to the DOA-dependent so-called steering vector $\mathbf{a}(\theta)$ whose m -th component is given by

$$[\mathbf{a}(\theta)]_m = g_m(\theta) \exp[j2\pi\rho_m \cos(\theta - \phi_m)]. \quad (1)$$

Sensor m is not necessarily omni-directional and $g_m(\theta)$ expresses the directive response of sensor m . For obvious practicality reasons, one unique type of sensors will be used with a different orientation at every sensor:

$$g_m(\theta) = g(\theta - \psi_m), \text{ for some angle } \psi_m.$$

A group of N such snapshots $(\mathbf{x}(t))_{t=t_1, \dots, t_N}$ is collected and used to estimate the DOA θ of the source. Given the plethora of estimation techniques, the CRB [9] is often used to evaluate the estimation accuracy, as it is algorithm-independent.

It, actually, represents the lowest MSE achievable by an unbiased estimator which is achieved (in the single source case) by many popular algorithms in practical systems [3]. Under the standard deterministic assumption, the CRB concentrated on the parameter θ only is compactly expressed as

$$\text{CRB}(\theta) = \frac{\sigma_n^2}{2N\sigma_s^2} F^{-1}(\theta),$$

where σ_s^2 and σ_n^2 denote, respectively, the signal and noise power and

$$F(\theta) = \|\mathbf{a}'(\theta)\|^2 - \frac{|\mathbf{a}^H(\theta)\mathbf{a}'(\theta)|^2}{\|\mathbf{a}(\theta)\|^2}, \quad (2)$$

is power-independent [8] with $\mathbf{a}'(\theta) \triangleq d\mathbf{a}(\theta)/d\theta$.

3. THE UCA ARRAY GEOMETRY

The UCA is made of $M \geq 3$ sensors placed uniformly along the circle, i.e. at angles $\phi_m = 2\pi(m-1)/M$, $m = 1, \dots, M$. The circle radius is $R\lambda$ where

$$R = \frac{\rho}{2 \sin\left(\frac{\pi}{M}\right)} \quad (3)$$

ensures a constant inter-sensors spacing equal to ρ , usually chosen in order to limit array ambiguities and/or inter-sensors coupling [4]. If the array is made of directional (very often symmetric as well) sensors, a problem arises about how to point the sensors. For the sake of isotropy, the main lobe is oriented in the direction opposite to the circle origin:

$$g_m(\theta) = g(\theta - \phi_m).$$

This design has been adopted in [4, 7, 6] but the assumption that the so-constructed array is isotropic is not supported by other than loose geometric argumentation. In this paper, we will remedy to this by a proper and rigorous analysis.

3.1. UCA of Symmetric Sensors

In practice, sensors response often verifies to be symmetrical (even) patterns $g(\theta)$, i.e.

$$g(\theta) = g(-\theta). \quad (4)$$

Added to the fact that response $g(\theta)$ is, by definition, 2π -periodic, we can write, without loss of generality,

$$g(\theta) = g_0 \left[1 + \sum_{k=1}^K b_k \cos(k\theta) \right], \quad (5)$$

where $(b_k)_{k=1, \dots, K}$ satisfy $1 + \sum_{k=1}^K b_k \cos(k\theta) \geq 0$ for all θ and also $b_1 \geq 0, \dots, b_{K-1} \geq 0$ and $b_K > 0$, hence assuring a maximum gain in the 0 [DEG] look direction.

By extensive use of the Euler relation

$$\sum_{m=1}^M \exp(jk\phi_m) = \begin{cases} M & \text{if } k/M \in \mathbb{Z} \\ 0 & \text{otherwise} \end{cases}, \quad (6)$$

we prove in Appendix 5.1 the following result.

Result 1 *If the directive sensors have symmetric responses satisfying (5), then the UCA made of M of such sensors is isotropic if $M > 2(K+1)$, with*

$$2 \frac{F(\theta)}{Mg_0^2} = \sum_{k=1}^K k^2 b_k^2 + \pi^2 R^2 (4 + b_1^2 - 4b_2\delta_{K \geq 2} + 2\delta_{K \geq 2} \sum_{k=2}^K b_k^2 - 2\delta_{K \geq 3} \sum_{l=3}^K b_{l-2}b_l) \quad (7)$$

where $\delta_A = 1$ if A is satisfied and 0, otherwise.

This result applies to the UCA of omni-directional sensors known to be isotropic if $M > 2$ [5]. This result proves that a UCA with directional sensors can still be isotropic if the number M of sensors is sufficiently large whatever their directivity.

Note that there is no direct relation between the directivity of the sensors defined as in [4] by

$$D = \frac{\max_{\theta} g^2(\theta)}{\frac{1}{2\pi} \int_0^{2\pi} g^2(\theta) d\theta}.$$

and the minimum number of sensors that enables the isotropy of the UCA, except for specific families of patterns. For example, for the radiation pattern

$$g_0(1 + \cos(\theta))^K$$

studied in [4], the minimal number $1 + 2(K+1)$ of sensors to assure isotropy increases with the directivity proved in Appendix 5.2 to be given by

$$D = \frac{2^{4K}}{\sum_{\ell=0}^K \frac{(2K)! 2^{2(K-\ell)}}{(\ell!)^2 (2(K-\ell))!}} \quad (8)$$

which gives for example:

K	1	2	3	4
D	2.66	3.66	4.43	5.68

If $M \leq 2(K+1)$, the UCA is no longer isotropic and the fluctuations of $F(\theta)$ (with θ) increase with the directivity of the sensors. This is illustrated in the next section for the cardioid sensors.

3.2. UCA of Cardioid Sensors

Cardioid sensors, of frequent use in acoustic systems [11], are ones that verify (5) with $K = 1$ thanks to a directive response of the form

$$g(\theta) = g_0[1 + \beta \cos(\theta)],$$

where $\beta \in [0, 1]$. Sensors directivity

$$D = \frac{2(1 + \beta)^2}{2 + \beta^2}$$

increases with β from 1 to $8/3$. By application of (7) in the Result 1, the UCA of cardioid sensors is isotropic if made of 5 or more sensors. Then, it verifies

$$F(\theta) = \frac{Mg_0^2}{2} [\beta^2 + \pi^2 R^2 (4 + \beta^2)],$$

consistently with the deterministic CRB for omni-directional sensors ($\beta = 0$) given in [5] as

$$\text{CRB}(\theta) = \frac{\sigma_n^2}{N\sigma_s^2} \frac{\sin^2(\frac{\pi}{M})}{\pi^2 M g_0^2 \rho^2}.$$

For completeness, in order to also address non-isotropic UCA of cardioid sensors, we prove in Appendix 5.3 the following expressions for arbitrarily sized UCA of cardioid sensors where R is given by (3)

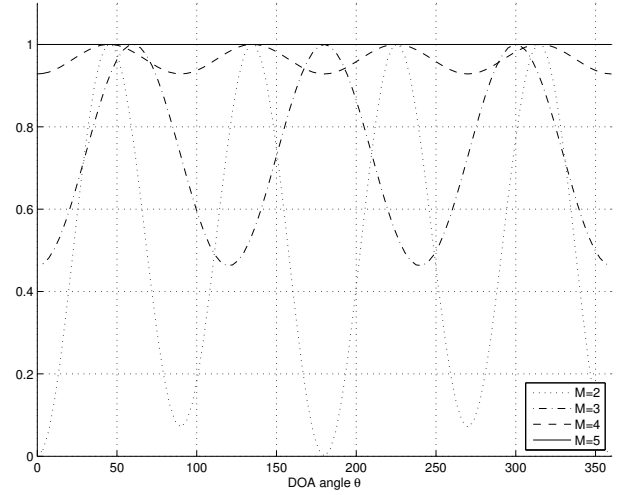
$$\begin{aligned} \frac{2F(\theta)}{g_0^2} &= \left\{ \beta^2 + \cos^2(\theta) [\pi^2 \rho^2 (4 + \beta^2) \right. \\ &\quad \left. - \beta^2 \frac{\beta^2 + 4\pi^2 \rho^2}{1 + \beta^2 \cos^2(\theta)}] \right\} 4 \sin^2(\theta), \quad M = 2 \quad (9) \end{aligned}$$

$$\begin{aligned} &= \pi^2 \rho^2 \left[4 + \beta^2 - 4\beta \cos(3\theta) - \frac{\beta^4 \sin^2(3\theta)}{2 + \beta^2} \right] \\ &+ 3\beta^2, \quad M = 3 \quad (10) \end{aligned}$$

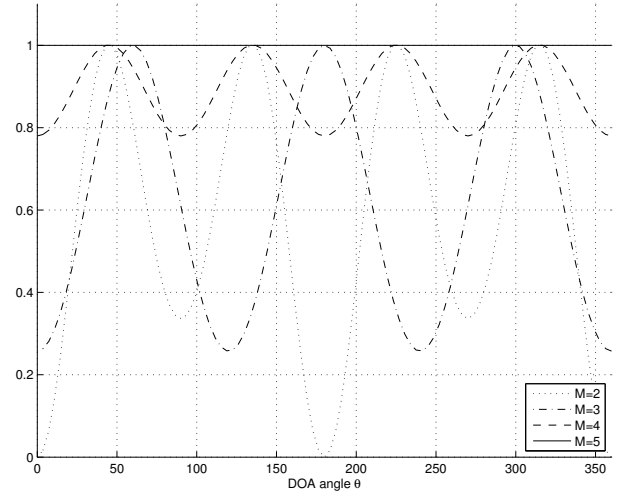
$$= 4\beta^2 + 4\pi^2 \rho^2 [2 + \beta^2 \sin^2(2\theta)], \quad M = 4 \quad (11)$$

$$= M \left[\beta^2 + \frac{\pi^2 \rho^2}{\sin^2(\frac{\pi}{M})} \left(1 + \frac{\beta^2}{4} \right) \right], \quad M > 4. \quad (12)$$

Dependence of $F(\theta)$ on the DOA angle θ is illustrated in Fig. 1. It shows that the UCA made of more directive sensors (i.e., with larger values of β) suffers larger fluctuations in its estimation accuracy. Notice that we should not forget that the larger fluctuations are compensated by larger absolute values of $F(\theta)$ (and smaller CRB), which can not be seen on the figure because of the normalization.



(a)



(b)

Fig. 1. $F(\theta)$ (which is inversely proportional to the CRB), normalized to its peak value $\max_{\theta}[F(\theta)]$, for all possible source DOAs. The UCA, whose size is shown in the legend, is made of cardioid sensors such that $\beta = 0.4$ in (a) and $\beta = 0.8$ in (b).

4. CONCLUSION

Contrarily to a widely-spread idea, UCAs are not systematically isotropic. They do not always exhibit the same DOA accuracy at all look directions. They are isotropic only starting from a minimum number of sensors. The minimum required number of sensors is obtained by (the order of) the Fourier series of the sensor response.

5. APPENDIX

5.1. Proof of Result 1

Rewriting (1) as $[\mathbf{a}(\theta)]_{m=1,\dots,M} = g_m \exp(j\tau_m)$, eq. (2) becomes:

$$F(\theta) = \frac{\sum_{m=1}^M g_m'^2 + \sum_{m=1}^M g_m^2 \tau_m'^2}{\sum_{m=1}^M g_m g_m'} + \frac{(\sum_{m=1}^M g_m g_m')^2 + (\sum_{m=1}^M g_m^2 \tau_m')^2}{\sum_{m=1}^M g_m^2},$$

with $g_m' \hat{=} dg_m/d\theta$ and $\tau_m' \hat{=} d\tau_m/d\theta$.

Euler identity (6) implies the following

$$\sum_{m=1}^M \sin[k(\theta - \phi_m)] = 0 \text{ for } M > k \geq 1$$

$$\sum_{m=1}^M \sin[k(\theta - \phi_m)] \cos[l(\theta - \phi_m)] = 0 \text{ for } M > k + l \geq 2$$

$$\sum_{m=1}^M \sin(\theta - \phi_m) \cos[k(\theta - \phi_m)] \cos[l(\theta - \phi_m)] = 0 \text{ for } M > 1 + k + l \geq 3,$$

which allow us to expand the sums

$$\left(\sum_{m=1}^M g_m g_m'\right)^2 \text{ and } \left(\sum_{m=1}^M g_m^2 \tau_m'\right)^2$$

and to prove, after simple algebraic manipulations that:

$$\begin{aligned} |\mathbf{a}^H(\theta)\mathbf{a}'(\theta)|^2 &= \left(\sum_{m=1}^M g_m g_m'\right)^2 + \left(\sum_{m=1}^M g_m^2 \tau_m'\right)^2 \\ &= 0 \text{ for } M > 2K + 1. \end{aligned}$$

Now, using the following equalities

$$\begin{aligned} \sum_{m=1}^M \sin[k(\theta - \phi_m)] \sin[l(\theta - \phi_m)] &= \sum_{m=1}^M \cos[k(\theta - \phi_m)] \cos[l(\theta - \phi_m)] \\ &= \begin{cases} M/2 & \text{for } M > k + l \geq 2 \text{ and } k = l \\ 0 & \text{for } M > k + l \geq 2 \text{ and } k \neq l \end{cases} \end{aligned}$$

$$\begin{aligned} \sum_{m=1}^M \cos[2(\theta - \phi_m)] \cos[k(\theta - \phi_m)] &= \begin{cases} M/2 & \text{for } M > k + 2 \geq 3 \text{ and } k = 2 \\ 0 & \text{for } M > k + 2 \geq 3 \text{ and } k \neq 2 \end{cases} \end{aligned}$$

$$\begin{aligned} \sum_{m=1}^M \cos[2(\theta - \phi_m)] \cos[k(\theta - \phi_m)] \cos[l(\theta - \phi_m)] &= \\ \begin{cases} M/4 & \text{for } M > k + l + 2 \geq 4 \text{ and } k = l = 1 \\ M/4 & \text{for } M > k + l + 2 \geq 4 \text{ and } |k - l| = 2 \\ 0 & \text{for } M > k + l + 2 \geq 4, |k - l| \neq 2, l \neq 1, k \neq 1 \end{cases}, \end{aligned}$$

we expand the two sums

$$\sum_{m=1}^M g_m'^2 \text{ and } \sum_{m=1}^M g_m^2 \tau_m'^2$$

to end the proof of Result 1.

5.2. Proof of the directivity (8)

Clearly $\max_{\theta} g_0^2(1 + \cos(\theta))^{2K} = 2^{2K} g_0^2$. Then applying two times the binomial equality to

$$(1 + \cos(\theta))^{2K} = \frac{1}{2^{2K}} [2 + (e^{j\theta} + e^{-j\theta})]^{2K},$$

we obtain:

$$(1 + \cos(\theta))^{2K} = \frac{1}{2^{2K}} \left[\sum_{k=0}^{2K} \sum_{\ell=0}^k 2^{2K-k} \binom{2K}{k} \binom{k}{\ell} e^{j(2l-k)\theta} \right].$$

Using the Euler relation (6),

$$\frac{1}{2\pi} \int_0^{2\pi} (1 + \cos(\theta))^{2K} d\theta = \frac{1}{2^{2K}} \sum_{n=0}^K 2^{2(K-n)} \binom{2K}{2n} \binom{2n}{n}$$

with $\binom{a}{b} \hat{=} \frac{a!}{b!(a-b)!}$ concludes the proof.

5.3. Proof of equalities (9)-(12)

Using again (6), we prove after tedious algebraic manipulations that

$$\begin{aligned} \frac{\|\mathbf{a}(\theta)\|^2}{M} &= g_0^2 + g_0^2 \beta^2 \frac{1 + \delta_{M,2} \cos(2\theta)}{2}, \\ -\mathbf{a}^H(\theta)\mathbf{a}'(\theta) &= 0, M > 3 \\ &= j \frac{3}{2} \pi R g_0^2 \beta^2 \sin(3\theta), M = 3 \\ &= g_0^2 \beta (\beta + 4j\pi R) \sin(2\theta), M = 2 \\ \frac{\|\mathbf{a}'(\theta)\|^2}{M} &= \frac{g_0^2 \beta^2}{2} + \pi^2 R^2 g_0^2 \left(2 + \frac{\beta^2}{2}\right), M \geq 5 \\ &= \frac{g_0^2 \beta^2}{2} + \pi^2 R^2 g_0^2 [2 + \beta^2 \sin^2(2\theta)], M = 4 \\ &= \frac{g_0^2 \beta^2}{2} + \pi^2 R^2 g_0^2 \left[2 + \frac{\beta^2}{2} - 2\beta \cos(3\theta)\right], M = 3 \\ &= g_0^2 \beta^2 \sin^2(\theta) + \pi^2 R^2 g_0^2 (4 + \beta^2) \sin^2(2\theta), M = 2 \end{aligned}$$

where $\delta_{ij} = 1$ if $i = j$, 0 otherwise. The above can be used to calculate $F(\theta)$, as expressed by (2), leading to the expressions (9-12).

6. REFERENCES

- [1] R. O. Schmidt, "Multiple emitter location and signal parameter estimation," *IEEE Trans. Antennas Propag.*, vol. AP-34, no. 3, pp. 276-280, Mar. 1986.
- [2] H. Gazzah and J.P. Delmas, "Spectral efficiency of beamforming-based parameter estimation in the single source case," in *Proc. Statistical Signal Processing Workshop (SSP)*, 2011, pp. 153-156.
- [3] F. Demmel, "Practical Aspects of Design and Application of Direction-Finding Systems," in "Classical and Modern Direction-of-Arrival Estimation," T. E. Tuncer, B. Friedlander (Ed.), Academic Press, 2009.
- [4] B. R. Jackson, S. Rajan, B. Liao, and S. Wang, "Direction of Arrival Estimation Using Directive Antennas in Uniform Circular Arrays," *IEEE Trans. Antennas and Propag.*, vol. 63, no. 2, pp. 736-747, Feb. 2015.
- [5] H. Gazzah and K. Abed-Meraim, "Optimum Ambiguity-free directional and omni-directional planar antenna arrays for DOA estimation," *IEEE Trans. Signal Process.*, vol. 57, no. 10, pp. 3942-3253, Oct. 2009.
- [6] M. Biguesh and S. Gazor, "On proper antenna pattern for a simple source detection and localization system," *IEEE Trans. Antennas and Propag.*, vol. 57, no. 4, pp. 1073-1080, Apr. 2009.
- [7] B. Liao, K.-M. Tsui and S.-C. Chan, "Frequency invariant uniform concentric circular arrays with directional elements," *IEEE Trans. Aerosp. Electron. Syst.*, vol. 49, no. 2, pp. 871-884, April 2013.
- [8] H. Gazzah and J.P. Delmas, "CRB Based-design of linear antenna Arrays for near-field source localization," *IEEE Trans. Antennas and Propag.*, vol. 62, no. 4, pp. 1965-1973, Apr. 2014.
- [9] B. Porat and B. Friedlander, "Analysis of the asymptotic relative efficiency of the MUSIC algorithm," *IEEE Trans. Acoust., Speech, Signal Process.*, vol. 36, no. 4, pp. 532-544, Apr. 1988.
- [10] H. Gazzah, J. P. Delmas and S. M. Jesus, "Improved direction finding using a maneuverable array of directional sensors," in *Proc. Int. Conf. Acoustics, Speech, Signal Processing (ICASSP)*, 2015, pp. 2799-2803.
- [11] L. del Val, A. Izquierdo, M. I. Jimenez, J. J. Villacorta and M. Raboso, "Analysis of Directive Sensor Influence on Array Beampatterns," in *Microwave and Millimeter Wave Technologies Modern UWB antennas and equipment*, I. Mini (Ed.), InTech, March 2010.